



Archaeological Ceramics Studied by Scanning Electron Microscopy

J. FROH

Fakultät Chemie, Elektronenmikroskopie, Technische Universität München, 85747 Garching, Germany

Abstract. The use of scanning electron microscopy combined with energy dispersive X-ray fluorescence analysis in studies of archaeological pottery is discussed. The methods are described and results of their application to studies of Precolumbian glossy black pottery from northern Peru are reported in some detail.

Key words: scanning electron microscopy, energy dispersive X-ray analysis, surface studies.

1. Introduction

Scanning electron microscopy (SEM) combined with energy dispersive X-ray analysis (EDX) is an excellent tool in many fields of science [1], and it has found many applications to problems of archaeological ceramics [2, 3]. It yields high-resolution images of ceramic surfaces, but the interior of sherds can equally well be studied when it is exposed, either as a polished section or as a fracture surface. SEM provides plastic pictures which can easily be interpreted in terms of structural details. When combined with the analysis of characteristic X-rays emitted from the sample, it also provides information on the element distribution in the sample surface.

To obtain a scanning electron micrograph, the sample surface is scanned line by line with a well-focussed beam of electrons having an energy somewhere in the range between about 0.5 and 30 keV. The interactions of these primary electrons with the specimen give rise to the emission of electrons and photons, most importantly of secondary electrons, backscattered electrons and X-rays. These carry information on the topography of the surface and the element distribution in the target. To obtain a picture of the studied surface, one uses the signal from the electron detector to modulate the intensity of the electron beam of a cathode ray tube synchronised with the scanning electron beam. Alternatively, the detector output can be digitised and fed directly into a computer for further processing and picture generation.

The scanning electron microscope allows the observation of very fine details with a lateral resolution down to the order of about a nanometre, which depends mainly on the spot size onto which the primary electron beam can be focussed

and, to a lesser extent, on properties of the target. SEM yields a surprisingly large depth of focus, and hence has good spacial imaging capabilities. The characteristic X-rays emitted when the target is bombarded with electrons yield element analyses for selected spots on the target surface, or they can be used to produce images of the distribution of certain elements in the target surface.

When the electrons of the primary electron beam penetrate into the target surface, they gradually lose energy, knock on other electrons and are deflected from their direction of incidence until they are either stopped or leave the target again through the surface. As a result, electrons with different energies up to the energy of the primary beam may leave the sample surface. Low-energy electrons leaving the surface with energies of up to about 50 eV are called *secondary electrons* since, in most cases, they are not electrons of the incident beam but electrons knocked out of regions close to the surface of the specimen by the impinging electrons. Electrons emerging with energies between about 50 eV and the energy of the incident beam are called *backscattered electrons* because they are, indeed, mainly electrons of the primary beam that were deflected by large angles in the target and eventually re-emerge from the target surface. Both kinds of emerging electrons may be used for image formation.

The depth of penetration of the primary electrons into the target depends on the beam energy and the density and element composition of the target. For the conditions of SEM, it is usually of the order of a few micrometres. The incident energetic electrons also give rise to the emission of both bremsstrahlung and characteristic X-rays emitted after electrons have been knocked out of inner shells of the target atoms. While the characteristic X-rays may be used for the identification of the elements present in the target surface, the bremsstrahlung is mainly obnoxious, since it causes a continuous background of X-rays that reduces the sensitivity of the detection of the characteristic radiation.

2. Methods in SEM

2.1. SECONDARY ELECTRON IMAGES

Secondary electrons are most widely used for image formation in scanning electron microscopy mainly for two reasons, both of which are related to their low energy of 50 eV or less. One is that, because of their low energy, they can efficiently be collected by applying a small positive potential to the detector, usually a secondary electron multiplier. More importantly, however, these low energy electrons emerge from a very thin surface layer of the specimen of about 10 nm thickness or even less. There the probe electron beam still has virtually the diameter to which it is focussed by the beam forming electron optics. Only these secondary electrons provide the optimum lateral resolution of about a nanometre. When the probe electron beam penetrates deeper into the target, it widens into a bulb-shaped distribution, whose maximum diameter is not much smaller than the maximum penetration depth. Secondary electrons are also ejected from a thin (≈ 10 nm) surface layer

by backscattered electrons when these emerge from the target surface. They then come from a much wider region with a diameter comparable to the penetration depth of the primary beam and hence of the order of a few micrometres. Therefore they contribute a rather blurred background, but fortunately their intensity is low and therefore this is usually not very disturbing.

Sharp scanning electron micrographs with resolutions down to about a nanometre are thus obtained with secondary electrons and carry information on the surface of the specimen down to a depth of at most about a nanometre. Owing to the large depth of focus of SEM images, sharp and plastic pictures of the studied specimens are obtained. These can quite easily be interpreted intuitively without much special knowledge. The brightness in these pictures is quite insensitive to the nature of the surface, e.g., to the elements it contains. It rather reflects properties of the target topography and the angle of the incident probe beam.

2.2. BACKSCATTERED ELECTRON IMAGES

Backscattered electrons emerge mainly at large angles to the target surface, and their directional distribution depends on the angle the probe beam forms with the target surface. They come mainly from depths inside the target down to about half the range of the primary beam, i.e., from depths of the order of a few micrometres. In these depths the primary probe beam has already widened to a micrometre size diameter, irrespective of how well it was focussed at the surface, but depending on the acceleration voltage. The lateral resolution of images obtained with backscattered electrons is therefore inferior to that of secondary electron images. One advantage of imaging with backscattered electrons is that a comparatively thick layer of about a micrometre contributes to the image formation. One thus can look below the surface layer probed by secondary electrons. Moreover, the backscattering efficiency increases with the atomic number Z of the elements in the probed layer, because backscattering is mainly caused by large-angle deflections of electrons in the electrostatic field of the target nuclei. Backscattered electron images therefore contain information on the element composition in addition to information on the topography of the specimen. The preferred specimens for investigations with backscattered electrons are polished surfaces of the objects to be studied, be they ceramics, mineral assemblages or metallurgical materials.

Because of their higher energy, backscattered electrons cannot be collected into the detector by applying a positive bias voltage to the latter as secondary electrons can be. One therefore must use rather large, appropriately positioned detectors, mostly scintillation detector elements or silicon p-n junction detectors. In modern instruments several detector segments are arranged around the probe electron beam. The output of these individual detectors can then be combined in different ways to obtain pictures that are mainly sensitive to the element distribution in the target or mainly sensitive to the target topography.

2.3. X-RAY ANALYSIS IN SCANNING ELECTRON MICROSCOPY

X-rays are produced whenever energetic electrons penetrate into a material. Depending on the emission process, one distinguishes between bremsstrahlung and characteristic X-rays. For element analysis by X-ray fluorescence, one makes use of the characteristic X-rays, whose energies are characteristic of the elements present in the target material. Characteristic X-rays are emitted when holes created by the probe electrons in the inner electron shells of target atoms are filled by electrons from outer shells. The energy, and hence the wavelength, of these X-rays depends, for any given atomic number Z , mainly on the electron shell in which the primary hole was created. One thus distinguishes K, L, M, etc., X-rays, which have energies decreasing in this order. Since the electron filling a hole may come from different higher shells, and owing to the fine structure of the electron energies within each shell, there are not one but several K, L, and M X-ray lines, and characteristic X-ray spectra of a single element already consist of several lines.

The energy of the individual X-rays depends in a systematic way on the atomic number Z of the emitting element. The energy of K X-rays, for instance, is to a good approximation proportional to Z^2 . Since holes can be created only in shells with binding energies less than the energy of the incident probe electron beam, X-rays emitted from the specimen in a scanning electron microscope will usually have energies of about 20 keV or less. On the other hand, the X-ray detectors used cannot detect radiation with energies much below 0.3 keV. In this energy bracket, one finds the K X-rays of the elements from C to Ru, the L X-rays for the elements above Ca, and the M X-rays of the elements above Nb. For the identification of individual elements in the SEM, one must therefore use the appropriate kind of X-rays [1, 4].

Bremsstrahlung is emitted whenever electrons are accelerated or decelerated. This happens to the probe electrons mainly in the electric field of the target nuclei. Bremsstrahlung has a continuous energy spectrum reaching up to the kinetic energy of the exciting electrons, independent of the nature of the target material. Bremsstrahlung is of no use in X-ray fluorescence analysis, but it gives rise to a continuous background that may render the detection of characteristic X-ray peaks more difficult. Since the intensity of bremsstrahlung emission increases with the atomic number Z of the elements in the target, the presence of heavy elements may reduce the detection sensitivity for light elements. The bremsstrahlung background may be automatically subtracted from the X-ray spectra by modern data processing routines, but it still impairs the detection limit of minor elements in the target. The intensity of bremsstrahlung in a given energy interval also increases with the probe acceleration voltage. For light elements, one may therefore optimise the detection limit by choosing an acceleration voltage that is high enough to excite the respective characteristic X-rays but does not produce unnecessarily much bremsstrahlung.

For the spectroscopy of X-rays in the SEM, two fundamentally different techniques are available, namely the so-called wavelength dispersive (WDX) and the energy dispersive (EDX) systems. A wavelength dispersive X-ray analyser consists of one or several crystal monochromators which, according to Bragg's law, select a certain wavelength from the spectrum of X-rays emitted by the target. Usually, several monochromators are used, each of which is set to a specific wavelength. One can then determine several elements at a time. For the actual detection of the X-rays one may, for instance, use a proportional counter. WDX systems have excellent wavelength – and hence energy – resolution, which often facilitates a quantitative evaluation for elements with close lying X-ray peaks. In the SEM, however, the moving spot from which the X-rays emerge, as well as rough surfaces or grainy structures cause collimation problems. WDX analysers are therefore rarely used in SEM systems. They are, however, a standard analytic device in electron microprobes, in which the focussed electron beam is mainly used for quantitative spotwise element analysis of polished sections of minerals and other materials [5].

Energy dispersive EDX spectrometres simultaneously measure the whole X-ray spectrum and hence provide a quick determination of the element composition of the target. Compared to WDX, the energy resolution is inferior, but tilted and rough surfaces and the movement of the emitting spot over the target surface do not adversely affect the X-ray analysis.

The detectors used in modern EDX systems are mainly lithium-drifted silicon semiconductor diodes, which have good energy resolution and detection efficiency for X-ray energies between a few hundred eV and 50 keV. Standard Si–Li detectors need to be cooled with liquid nitrogen to reduce thermal noise, but recently detector systems became available which can do with cooling by Peltier elements. When an X-ray photon is absorbed in the detector, a voltage pulse with a height proportional to the X-ray energy is produced. These pulses are digitised in an analog-to-digital converter (ADC) and stored in a multichannel counter, which yields a pulse height or energy spectrum of all X-ray lines simultaneously. The lines in this spectrum can be analysed in terms of the individual elements present in the spot on the specimen hit by the electron beam.

For modern EDX systems the detection limit for most elements is of the order of 0.1 mass percent, but it varies considerably with the target material, the acceleration voltage of the electron beam and the angle of electron incidence on the target. The acceleration voltage should be between 15 and 30 kV to facilitate the simultaneous detection of light and heavy elements. Quantitative determinations of individual elements require that the attenuation of the primary beam in the target as well as the absorption of the X-rays in the target material be taken into account, which requires an *a priori* knowledge of the target composition and hence tedious iterative calculations [1, 6]. The software of modern EDX systems permits such determinations, but in practice inhomogeneities and a complicated topography of the target surface may severely limit the accuracy.

The signal of the characteristic X-rays of specific elements may also be used for picture formation. One then obtains maps of the distribution of certain elements in the target surface. Modern computing facilities permit one to take such pictures of several elements simultaneously with a resolution comparable to that obtained in backscattered electron pictures.

The usefulness of EDX in studies of ceramics is illustrated by Figures 1 and 2, which show the secondary electron micrograph and several EDX patterns of a fresh fracture surface of a piece of Celtic ware from the oppidum of Manching in southern Germany. This type of ceramics has been studied in some detail by neutron activation analysis, Mössbauer spectroscopy, optical thin section microscopy and X-ray diffraction. These studies are reviewed in a separate paper in this volume [7]. The micrograph of Figure 1 shows the morphology of the fine grained clay matrix and some rather large inclusions, but it is difficult to identify the nature of the latter because they exhibit no idiomorphic crystal faces. The inclusions can, however, be identified with the help of EDX. The three EDX spectra shown in Figure 2 are of the clay matrix, of an inclusion identified as quartz, and of one that can be identified as a sodium feldspar. All patterns show the X-ray peaks of oxygen and silicon. The quartz (SiO_2) shows practically nothing else, while the inclusion identified as a feldspar additionally exhibits the lines of Na, Al, and very little K. Most probably, it is a sodium feldspar, $\text{Na}[\text{AlSi}_3\text{O}_8]$, of the albite–orthoclase system. The clay matrix contains much aluminium, some potassium and a little iron. This tallies well with the illitic clay from which the Celtic pottery from Manching was made [7].

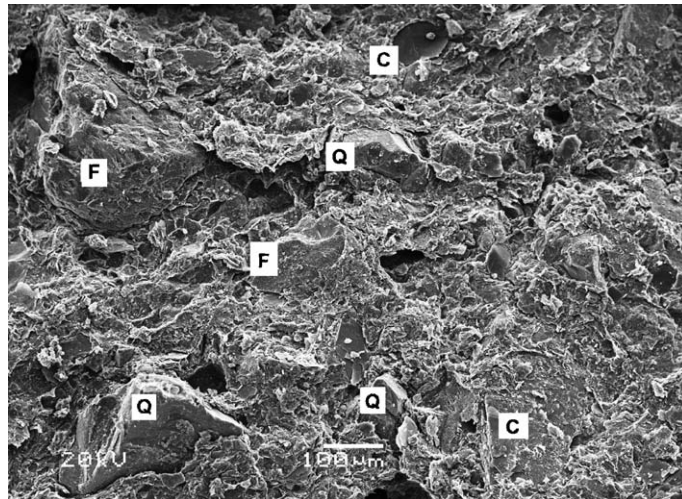


Figure 1. Scanning electron micrograph of a fresh fracture surface through a Celtic sherd from Manching showing the clay matrix and several sizeable crystalline inclusions, which were identified by EDX. The letters mean C – clay, Q – quartz, and F – feldspar.

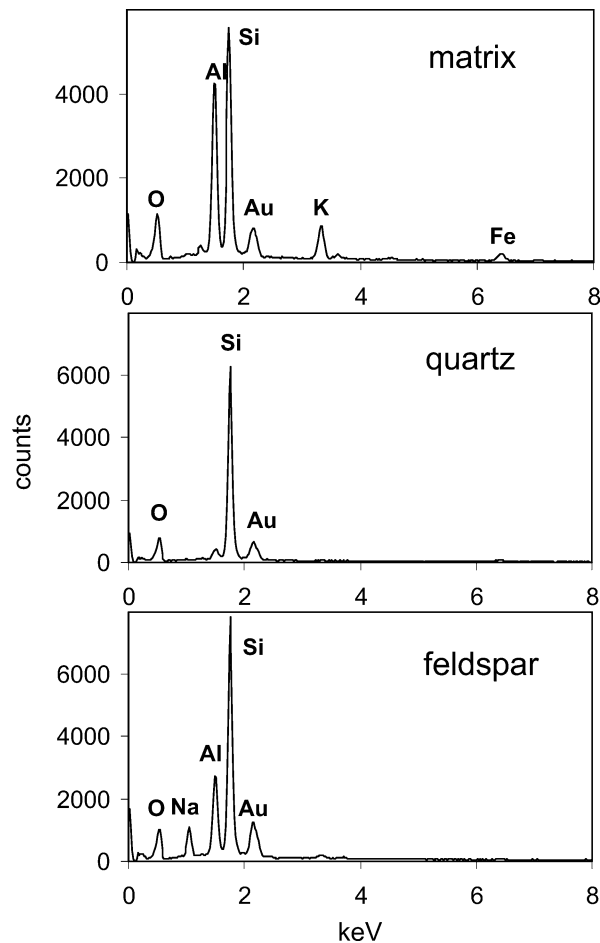


Figure 2. EDX spectra of three individual spots in the micrograph of Figure 1 representing the clay matrix, quartz and feldspar. The elements to which the X-ray lines belong are noted in the spectra. Gold (Au) is always present because the specimen was coated with a conducting layer of this element.

2.4. SAMPLE PREPARATION

Since only a fraction of the electron charge incident on the target in the SEM is re-emitted as backscattered or secondary electrons, the excess charge must be carried off to the metallic target holder. This is no problem for electrically conducting specimens, but insulating ones like ceramics need to be covered by a thin conducting surface layer. To this end, one usually deposits a 1–10 nm thick conducting film onto the target. The most commonly used method is sputtering with gold or carbon in an argon atmosphere [8]. Other metals, like Pt or Au–Pd alloys, may also be used. In this way, a uniformly conducting cover is formed, which also reduces heating by the electron beam. This film is usually too thin to be, as such, seen in the micrographs, but it contributes to the emission of secondary electrons, which

is not very disturbing as long as it reflects the topography of the target. It does, however, tend to wipe out whatever little influence of the sample composition on the brightness in secondary electron micrographs may exist.

For studies of ceramics in the SEM one will usually use small fragments of sherds attached to the target holder by a conducting glue. Since the samples are to be studied in high vacuum, careful drying of the samples in a vacuum drying oven is recommended in order to avoid outgassing in the SEM as much as possible. Some modern SEMs can work with rather low vacuum, which alleviates this problem. Whether whole ceramic objects can be studied non-destructively depends on the size of the vacuum chamber available. SEMs with chambers large enough to accommodate and position sizeable objects exist, but are still not very common.

Secondary electron SEM images of the ceramic surface and of fresh fracture surfaces give good high resolution pictures of the surface topography, of slips and of the bulk of the ceramic paste. Backscattered electron micrographs of polished sections yield poorer resolution but information on the element distribution in the target, since heavy elements produce more secondary electrons than light ones. Secondary electron micrographs of polished sections are of little use, since they would mainly reflect the surface structure caused by polishing. Oblique views of fracture zones more or less perpendicular to the surface allow one to see the surface and the region below the surface of a sherd in the same picture. This will, for instance, reveal the application of slips and other surface treatments, for whose study scanning electron microscopy with EDX element analysis is particularly well suited [9]. It largely depends on the desired information whether polished sections or untreated surfaces and fracture zones are preferable.

3. Archaeological applications

Applications of scanning electron microscopy to pottery and ceramics are manifold. The impact of SEM and X-ray microprobe analysis on ceramic studies has been reviewed by Tite [3], who mentions mainly three types of information that can be obtained from SEM: information on the raw materials used, information on firing procedures, and information on surface decoration, i.e., the application and nature of slips and glazes.

Most applications made use of polished sections, often sections perpendicular to the surface. SEM has the advantage of better resolution than optical thin section microscopy under a polarising microscope, but the disadvantage that the identification of individual mineral phases is more difficult. SEM using backscattered electrons is therefore often preferred to secondary electron micrographs, because of its sensitivity to the mean atomic number of individual phases, which allows at least a rough identification. Information on the firing temperature, for instance, can be obtained from the presence or absence of vitrification.

A fine example is a study of the high gloss surfaces of Greek Attic and Roman Samian ware [10], two types of pottery that are both important in archaeology

and interesting from the scientific point of view. The Greek Attic ware is famous for its glossy black and red surface decorations. According to Tite *et al.* [10], the red and black parts of the surface were obtained by first firing in a reducing and then in an oxidising kiln atmosphere. During the reducing firing stage, the Fe^{3+} in the iron-rich slips, containing about 12 wt.% of iron as determined by EDX analysis [10], is converted to Fe^{2+} in a spinel phase of the magnetite–hercynite solid solution type. During the subsequent oxidising firing stage, the iron in the spinel phase was converted back to Fe^{3+} in hematite in the glossy red parts of the surface, while it remained in the spinel phase as Fe^{2+} in the glossy black parts. This difference in behaviour is due to the different porosities of the red and black surface layers, which are well seen in the scanning electron micrographs. The more porous red slip allowed the penetration of oxygen during the final firing stage and hence the re-oxidation of the iron, while the less porous black one did not. The element composition of the red and black slip is, however, practically the same, indicating that a mixture of iron oxide and an illitic clay was used for painting. The reason for the black gloss having a denser and more thoroughly vitrified texture than the red one seems to lie purely in the grain size of the raw materials. Possibly, the starting material was a single clay, the same that was used also for the bodies of the ceramics. From this, two fine fractions seem to have been separated, the one finally giving the black surface being even finer than the one giving the red surface owing to its higher permeability to oxygen during the final, oxidising firing stage.

Studies of surfaces, glazes and slips are probably the most promising field of application of SEM in ceramic studies, as some recent studies show [9, 11]. In the following, an example concerning the black surfaces of Precolumbian ceramics from Peru will be given. Ceramics with glossy black surfaces are frequent in the Sicán culture of northern Peru [12–14]. The question what causes these black surface and how this type of blackware ceramics was made has been addressed both by studies of the ancient pottery and by field firing experiments in an ancient kiln at the excavation site. In these experiments, replicas of blackware ceramics, very similar to the ancient finds were produced. Both ancient and replica blackware was studied by Mössbauer spectroscopy, X-ray diffraction, optical thin section microscopy and scanning electron microscopy [12]. Some results of the latter method are reported here as an example of the kind of information that may be gleaned from SEM combined with EDX. The instrument used in these experiments was a Jeol SEM-5900 scanning electron microscope operated at an accelerating voltage of 20 kV and combined with a Röntec EDX analyser. To expose the surface layer as well as the interior of the sherds, fresh fracture edges perpendicular to the surfaces were looked at under an oblique angle so that both the surface and the fracture plane can be seen in one micrograph.

One ancient and two replica sherds were studied. The ancient sherd is registered under the number 39/88 in the archaeological data base at Garching, while the two studied replica sherds have the numbers 39/323 and 39/324. Both the ancient and the replica pieces have shiny black surfaces that were supposed to be caused by

carbon deposits formed during the reducing firing. Apparently, no slip was applied to the ancient blackware pottery. In the production of the replica pottery, no slip was applied either, but the surface of the leather dried vessels was very carefully burnished before firing. This was found to be of great importance for obtaining a glossy black surface after reducing firing. The firing of the replica pottery in an ancient kiln at Batán Grande is described in [13]. Scanning electron microscopy and EDX analysis were performed on both the ancient and the replica sherds in order to elucidate the nature of the carbon deposits causing the black surfaces.

Figure 3 shows electron micrographs of oblique fracture edges of black sherds with a glossy surface. The micrograph on top is of replica sherd 39/323, while

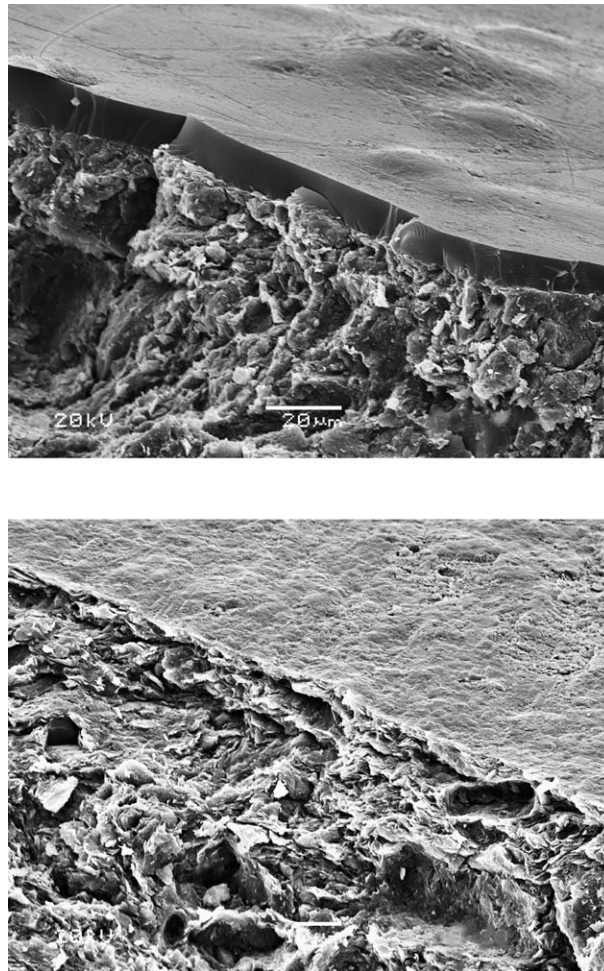


Figure 3. Scanning electron micrographs giving an oblique view of fresh fracture edges of a piece of replica ceramics with a glossy black surface (39/323, *top*) and of an ancient sherd of Sicán blackware (39/88, *below*).

the one below is of the piece of ancient blackware ceramics (39/88). The replica exhibits a continuous, smooth surface layer with a thickness between 5 and 10 μm on top of the fractured clay matrix. The surface of the ancient sherd is also rather smooth, but rougher than that of the replica and only a few μm thick, although visually both sherds appear glossy black. The roughness of the surface of the ancient sherd may be due to weathering or to less perfect burnishing. It probably was never covered with a smooth continuous surface layer like to one seen on the replica. The micrograph does, however, show clearly that no slip was applied to the ancient sherd.

In Figure 4 a micrograph of the fracture edge of the replica sherd is shown together with EDX spectra of the surface layer and of a spot in the clay matrix, about 12 μm below the surface. The gold M X-rays in both cases arise from the gold coating of the sample. In the surface layer, the K X-rays of carbon are predominant, whereas 12 μm below the surface, carbon is seen only very weakly. The major constituent elements of ceramics, silicon, aluminium, and oxygen, are now predominant. The other elements usually found in ceramics, Mg, K, Ca, and Fe are also well visible. This shows that the surface layer is mainly made up of carbon, which is nearly absent already some 12 μm below the surface. The weak Si, Al, and O peaks in the surface layer are probably due to particles from the clay matrix adhering to the fracture zone. The small amount of carbon observed in the interior of the sherd may be due to penetration of carbon into the sherd during firing.

The EDX spectra of the sherd of ancient blackware (Figure 5) are similar to those of the replica. The carbon line is still predominant in the surface layer, but the elements typical for clay are stronger than for the surface of the replica, presumably because the carbon layer, although well visible in the micrograph, is much thinner than on the replica, and therefore the spot of the EDX analysis also covered some of the clay matrix. About 10 μm below the surface the carbon line is weaker than that of Si, but considerably stronger than in the case of the replica. Apparently, in the ancient sherd carbon has penetrated farther into the clay matrix, and is less concentrated in the surface layer, perhaps because the surface was less carefully burnished and hence less dense in the first place. The dense and smooth carbon layer on the replica suggests that the carbon was not deposited as soot particles but rather by pyrolytic decomposition of hydrocarbons contained in the kiln atmosphere on the very surface of the hot vessel.

Both for the replicas and the ancient blackware pottery, the X-ray analysis confirms that carbon is the prime cause of the black surfaces, though the micrographs show that there are substantial differences in the structure and thickness of the black surface coating.

The interior of the replica and of the ancient sherd are similar in texture and grain size, as can be seen from Figures 3 to 5. The clay platelets with sizes of several μm are well visible, which shows that the maximum firing temperature was not high enough to destroy their morphology, which is supposed to occur above

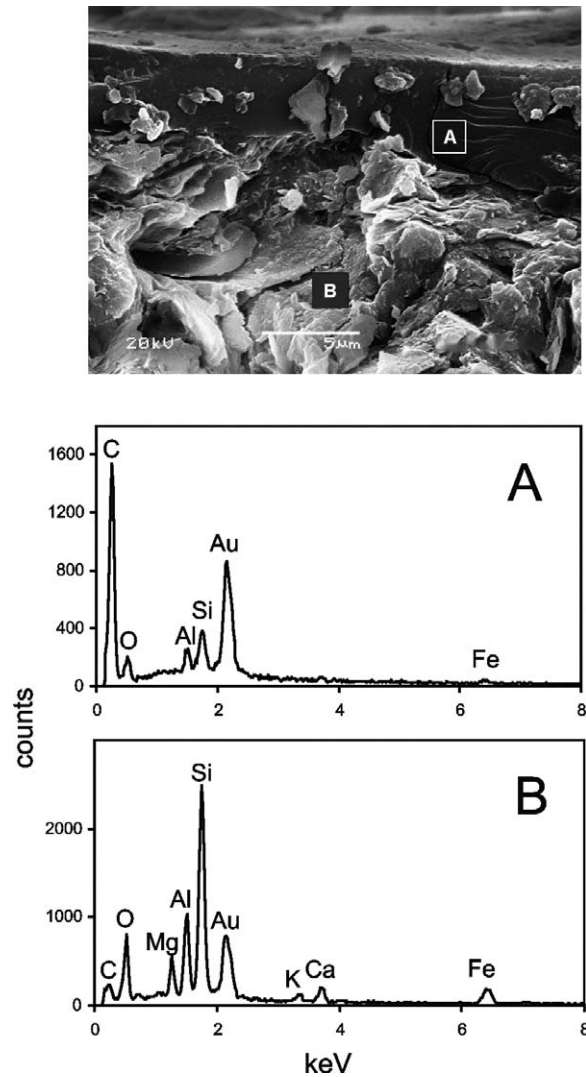


Figure 4. Scanning electron micrograph of a fresh fracture edge of replica blackware 39/323 and EDX spectra of a point in the surface layer (A) and in the interior (B). The glossy black surface layer shows a strong peak of carbon K X-rays at 0.28 keV, which are nearly absent in the interior of the sherd. The M X-rays of Au at about 2.2 keV arise from the gold coating of the specimen.

850°C [12, 13]. The platelets do, however, appear to be better oriented parallel to the surface in the replica than in the ancient sherd. This again indicates that the replica was better burnished prior to firing than the ancient sherd.

In Figure 6 perpendicular views onto the surfaces of the replica 39/324 are shown. The micrograph on top is of the glossy black outer surface, while the micrograph below shows the surface facing towards the interior of the vessel, which had not been burnished and is therefore comparatively rough. The outer surface

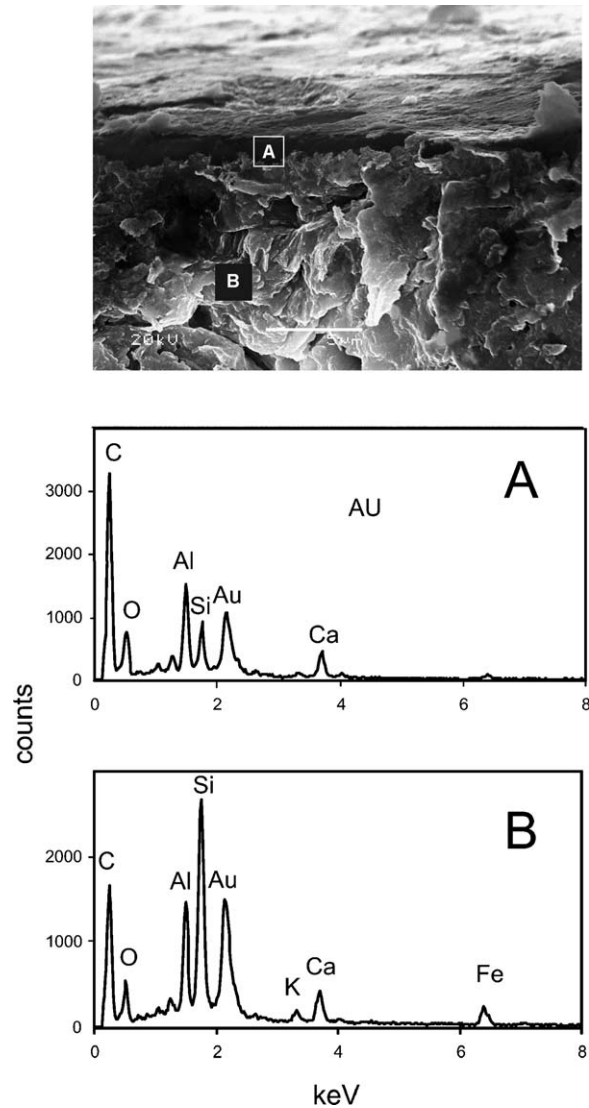


Figure 5. Scanning electron micrograph of a fresh fracture edge of a piece of ancient blackware pottery (39/88) and EDX spectra of a point in the thin black surface layer (A) and the interior of the sherd. The surface shows a stronger peak of carbon K X-rays at 0.28 keV than the interior of the sherd (B), but the carbon peak is substantial in both cases. The M X-rays of Au at about 2.2 keV arise from the gold coating of the specimen.

is glossy black, while the inner one is brown. The different surface textures are nicely seen in the electron micrographs. EDX spectra show practically no carbon on the inner surface, but carbon as the predominant element in the glossy black outer surface. Obviously no carbon was deposited on the inner surface, probably

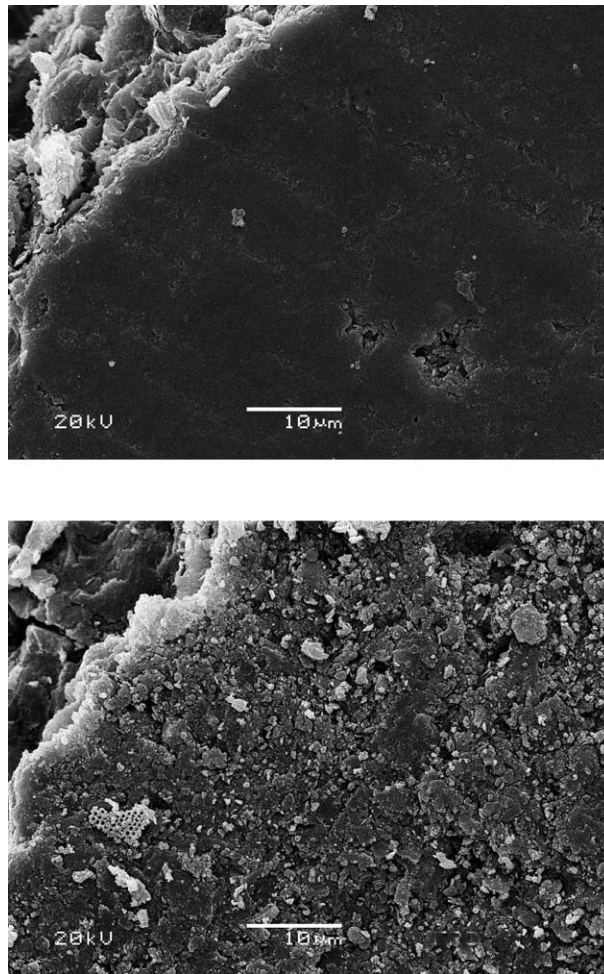


Figure 6. Scanning electron micrographs of the outer (*top*) and the interior (*bottom*) surface of replica vessel 39/324 with a glossy black outer and a dull brown interior surface. In both cases there are fracture edges in the upper left corner.

because the flue gases carrying the hydrocarbons that decomposed on the outer surface did not penetrate into the interior of the vessel.

In Figure 7 the black outer surface of the ancient blackware (39/88, *top*) is compared with that of the outer surface of the well burnished replica sherd (39/324, *below*) at a higher magnification than that of Figure 6. The coarser structure of the ancient sherd is clearly seen, although visually both appear very similar.

Finally, Figure 8 shows a perpendicular view onto the surface of the replica sherd in which several hexagonal particles can be seen lying with their faces in the plane of the surface. These were suspected of being crystalline graphite, which may form at relatively high temperatures, though most of the carbon layer apparently remains amorphous. The EDX spectrum of one of these hexagonal structures shows

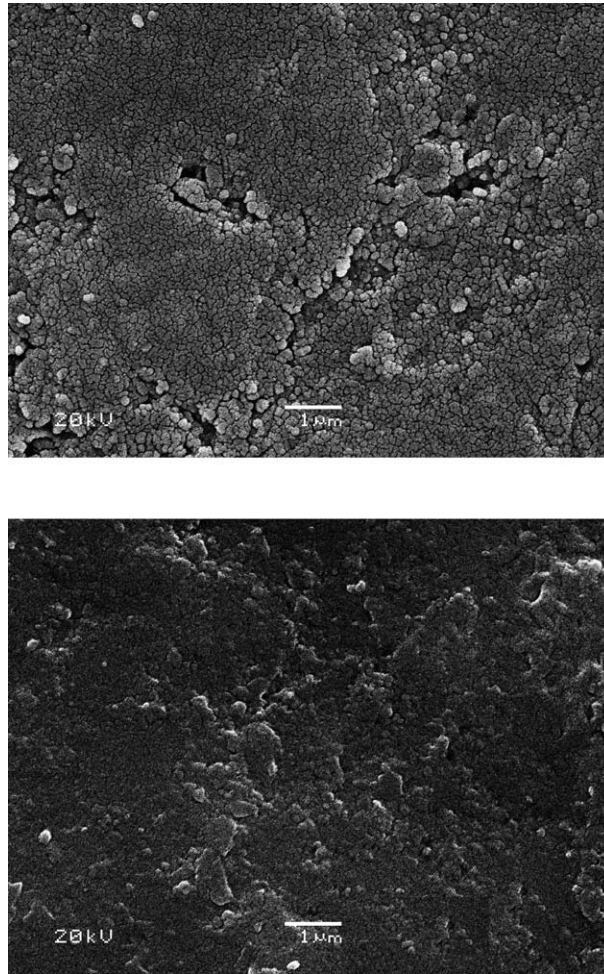


Figure 7. Glossy black surface of an ancient sherd of blackware (39/88, *top*) and of a replica sherd (39/324, *bottom*). Note that the magnification is higher than in Figure 6.

practically only carbon, with some additional oxygen (Figure 8). In this case, the gold M X-rays are absent because, relying on the electrical conductivity of the carbon surface layer, the specimen was not covered with a conducting gold layer.

The analyses of the outer and fracture surfaces confirm that the glossy black surface layer on the replica ceramics is due to carbon. X-ray diffraction has shown [15] that crystalline graphite is only a minor constituent of the surface layer. The black layer thus must therefore be mainly amorphous carbon and probably originated by pyrolysis of organic vapours in the kiln atmosphere when the kiln is operated with no or little admission of air. This idea is corroborated by the presence of a 5–10 μm homogeneous and continuous layer of carbon with no visible structure except for occasional hexagonal objects on the surface, which apparently represent

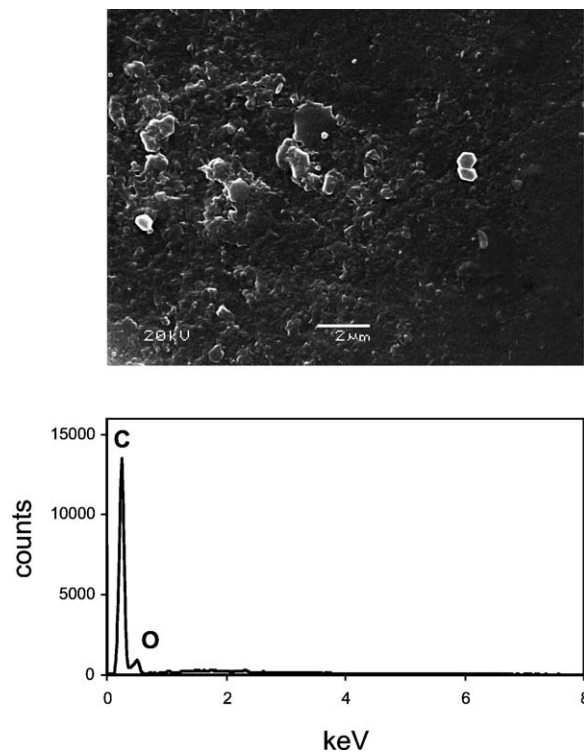


Figure 8. Scanning electron micrograph of the polished black surface of replica sherd 24/136 showing several hexagonal platelets (*top*) and an EDX spectrum taken on such a hexagonal platelet. The surface was not sputtered with gold, hence the Au M X-rays are absent.

the crystalline graphite observed in X-ray diffraction. In the case of the ancient sherd (Figures 3 and 5), EDX shows that carbon is also present in considerable amounts in the surface layer, but it does not form a thick, continuous layer like on the replica, although an indication of an amorphous carbon layer about a micrometer thick is also seen on the surface of the ancient sherd in Figure 5. On the other hand, carbon has penetrated deeper into the ancient sherd than into the replica.

The micrographs show that no slip was applied to the ancient blackware sherd. Consequently, one cannot expect magnetite or magnetite–hercynite solid solutions, which are important constituents of ancient greek black ceramics [10, 16, 17], to play any role in the case of the ancient Sicán blackware. This is confirmed by the EDX spectra of the blackware surface, which does not show any iron enrichment in the surface as would be expected if magnetite was present.

The differences in the morphology of the carbon layer on the surface of the ancient and replica blackware ceramics may be due to a different surface structure present already before firing, e.g., if the burnishing in the leather dried state was done more or less carefully. The firing conditions, however, may also have a profound influence on the state of the deposited carbon. It will, for instance, be of

importance whether carbon nanoparticles form already in the kiln atmosphere and are then deposited on the ceramic surface, or whether hydrocarbons decompose on the hot ceramic surface itself. In the latter case, the temperature of the surface at the time of decomposition may play an important, though as yet unexplored, role. To obtain more reliable information on this, additional laboratory experiments would need to be done.

4. Conclusions

The examples show that scanning electron micrographs yield detailed information on the structures of both surfaces and the paste of ceramic materials. In addition, EDX analysis provides information on the position-resolved element composition of the specimens. The particulate composition can then easily be interpreted, at least as long as the minerals in question are simple ones, like quartz or carbonates. Complex minerals like feldspars or clays cannot easily be identified by their element composition, but may be identified by their morphology in conjunction with EDX data. Still, the identification of individual minerals in ceramics may sometimes not be easy in the SEM alone. Additional data from XRD [15] and optical microscopy of thin or polished sections [18] will then be helpful to obtain a complete picture of the studied material.

References

1. Goldstein, J. I., Newbury, D. E., Joy, D. C., Lyman, C. E., Echlin, P., Lifshin, E., Sawyer, L. C. and Michael, J. R., *Scanning Electron Microscopy and X-ray Microanalysis*, 3rd edn, Kluwer Academic/Plenum, New York, 2003, ISBN 0-306-47292-9.
2. Tite, M. S., Freestone, I. C., Meeks, N. D. and Bimson, M., The Use of Scanning Electron Microscopy in the Technological Examination of Ancient Ceramics, In: A. D. Franklin and J. Olin (eds.), *Ceramics as Archaeological Material*, Smithsonian Institution Press, Washington, 1982, pp. 109–120.
3. Tite, M. S., The Impact of Electron Microscopy on Ceramic Studies, *Proceedings of the British Academy* **22** (1992), 111–131.
4. Birks, L., *Electron Probe Microanalysis*, Interscience, New York, 1963.
5. Venables, J. A., Electron Microscopy of Surfaces, *Ultramicroscopy* **7** (1981), 81–99.
6. Eggert, F. and Heckel, J., Die standardfreie quantitative Analyse auf der Basis der lokalen Peak/Untergrund Verhältnisse mit einem energiedispersiven Röntgenmicroanalysator EDR-184, *Exp. Technik d. Phys.* **34**(3) (1986), 201–211.
7. Gebhard, R., Bott, R. D., Distler, N., Michalek, J., Riederer, J., Wagner, F. E. and Wagner, U., Ceramics from the Celtic Oppidum of Manching and its Influence in Central Europe, In: U. Wagner (ed.), *Mössbauer Spectroscopy in Archaeology, Hyp. Interact.*, topical issue, Vol. 1, Kluwer.
8. Treiber, E., Beitrag zur Präparierung nicht leitender Objekte für die Rasterelektronenmikroskopie, *Mikroskopica Acta* **71/72** (1971), 242–249.
9. Mason, R. B., Tite, M. S., Paynter, S. and Salter, C., Advances in Polychrome Ceramics in the Islamic World of the 12th Century AD, *Archaeometry* **43**(2) (2001), 191–209.
10. Tite, M. S., Bimson, M. and Freestone, I. C., An Examination of the High Gloss Surface Finishes on Greek Attic and Roman Samian Wares, *Archaeometry* **24** (1982), 117–126.

11. Pérez-Arategui, J. and Castillo, J. R., Characterization of Red Coloured slips (Almagra) on Islamic Ceramics in Muslim Spain, *Archaeometry* **42** (2000), 119–128.
12. Shimada, I. and Wagner, U., Peruvian Black Pottery Production and Metalworking: A Middle Sicán Craft Workshop at Huaca Sialupe, *MRS Bull.* **26**(1) (2001), 25–30.
13. Shimada, I., Goldstein, D., Häusler, W., Sosa, J., Riederer, J. and Wagner, U., Early Pottery Making in Northern Coastal Peru. Part II: Field Firing Experiments, In: U. Wagner (ed.), *Mössbauer Spectroscopy in Archaeology, Hyp. Interact.*, topical issue, Vol. 2, Kluwer.
14. Shimada, I., Häusler, W., Jakob, M., Montenegro, J., Riederer, J. and Wagner, U., Early Pottery Making in Northern Coastal Peru. Part IV: Mössbauer Study of Ceramics from Huaca Sialupe, In: U. Wagner (ed.), *Mössbauer Spectroscopy in Archaeology, Hyp. Interact.*, topical issue, Vol. 2, Kluwer.
15. Stanjek, H. and Häusler, W., Basics of X-ray Diffraction, In: U. Wagner (ed.), *Mössbauer Spectroscopy in Archaeology, Hyp. Interact.*, topical issue, Vol. 1, Kluwer.
16. Maniatis, Y., Aloupi, E. and Stalios, A. D., New Evidence for the Nature of the Attic Black Gloss, *Archaeometry* **35** (1993), 23–34.
17. Maggetti, M., Galetti, G., Schwander, H., Picon, M. and Wessiken, R., Campanian Pottery, the Nature of the Black Coating, *Archaeometry* **23**(2) (1981), 199–207.
18. Riederer, J., Thin Section Microscopy Applied to the Study of Archaeological Ceramics, In: U. Wagner (ed.), *Mössbauer Spectroscopy in Archaeology, Hyp. Interact.*, topical issue, Vol. 1, Kluwer.